Self-similarities in one-dimensional periodic and quasiperiodic systems

T. Odagaki
Department of Physics, Brandeis University, Waltham, Massachusetts 02254

Hideaki Aoyama*
Department of Physics, Northeastern University, Boston, Massachusetts 02115
(Received 11 August 1988)

We find hyperinflation rules for periodic and quasiperiodic systems in one dimension which consist of two components and are characterized by a single-parameter α. Applying hyperinflation rules, we analyze the diffraction pattern and physical properties described by a class of transfer matrices in $SL(2,C)$. We show that the diffraction pattern is self-similar in the wave-vector–α space. We also show that the product of transfer matrices has self-similar structure in its asymptotic behavior in the space spanned by α and parameters in the matrices, which gives rise to self-similarity in various physical properties such as transmission coefficient, conductivity, heat conductivity, effective impedance, and spectral diffusion. Possible experiments are also discussed.

I. INTRODUCTION

Quasiperiodic one-dimensional systems have been studied not only from theoretical interest but also in connection with various physical situations. One of the well-known examples is the motion of a Bloch electron in a two-dimensional space perpendicular to a uniform magnetic field.[1] Quasicrystals proposed recently as a possible structure of certain quenched alloys[2–4] provide a quasiperiodic one-dimensional sequence of atoms in three-dimensional crystals. One-dimensional periodicity and quasiperiodicity have also been made in a quantum heterostructure[5] where two different materials are grown in a specified order with precise thickness. Furthermore, compactification in the string theory has been treated using ideas of quasicrystals.[6]

One of the simplest ways to produce periodic and quasiperiodic sequence is to use the projection method.[7] For example, if one projects a strip in a square lattice on to a line with slope ρ, one obtains lattice points at

$$x_n = n + \phi + \rho[\alpha n + \beta] , \tag{1.1}$$

where α, β, ρ, and ϕ are the parameters and [ ] denotes the Gauss symbol. (ϕ can be set to zero and α can be restricted in [0,1] without loss of generality.) We restrict our discussion in this paper to the case $\beta=0$ for simplicity. When α is a rational number, $\{x_n\}$ forms a periodic lattice and when α is an irrational number, the sequence of the points becomes quasiperiodic. Thus, one can produce infinitely many sequences by changing the parameter α.

In a previous Letter,[8] we introduced hyperinflation rules which relate sequences characterized by different α's. Various physical properties of one-dimensional systems defined by the sequence show self-similarity due to this symmetry. The hyperinflation rule is generally different from the inflation (deflation) rule known in certain quasiperiodic chains, since the latter is a transformation in β with a fixed α in Eq. (1.1),[9] while the former is a transformation in α keeping β constant.

The purpose of this paper is to study fully the consequences of the hyperinflation rules in physical properties of one-dimensional systems. We investigate the diffraction pattern of the sequence and the physical properties of the systems described by transfer matrices which are unimodular 2×2 matrices $[SL(2,C)]$. In Sec. II, we prove the existence of hyperinflation rules in periodic and quasiperiodic sequences. We obtain three essentially different rules. In Sec. III, we apply some of the rules to diffraction patterns and explain self-similar structures in the diffraction patterns in the (k,α) plane, k being the wave vector. As is briefly summarized in the Appendix, many physical systems can be described by $SL(2,C)$, which include a tightly bound electron, lattice vibration, hopping conduction, series of lenses, and two port circuits. The behavior of the product of $SL(2,C)$ determines physical properties such as localization, transmission coefficient, heat conductivity, staying probability, effective focal length, and effective impedance. In Sec. IV, we analyze numerically convergence of the product in the plane spanned by α and parameters in $SL(2,C)$, taking prototype matrices relevant to a tightly bound electron, lattice vibration, a sequence of lenses, and the Kronig-Penny model. We also analyze the self-similar structure in detail for matrices relevant to the Schrödinger equation using the hyperinflation symmetry. Discussion is given in Sec. V and we suggest possible experiments.

II. HYPERINFLATION

There are two spacings $a_0=1$ and $a_1=1+\rho$ in the lattice made by Eq. (1.1). A sequence of two components can be generated by assigning these two objects to the two different spacings. For simplicity, we set $\beta=0$ and consider the sequence of 0 and 1 given by

$$S_\alpha(k)\equiv[\alpha(k+1)]-[\alpha k], \quad k=1,2,3,\ldots . \tag{2.1}$$

First, we note that

$$S_\alpha(k)=\begin{cases}0 \text{ if } 0\le \exists i<k \text{ such that } \alpha\in[i/k,(i+1)/(k+1))\ ,\\ 1 \text{ if } 0<\exists i\le k \text{ such that } \alpha\in[i/(k+1),i/k)\ ,\end{cases} \tag{2.2}$$

where the value of i is uniquely determined for each case. Thus for a given 0 or 1, we can associate a parameter (k,i) by this equation. Now, we consider a Möbius transformation of α,

$$\alpha'=\frac{r\alpha+s}{u\alpha+v}\equiv f(\alpha)\ , \tag{2.3}$$

where r, s, u, and v are integers. We assume $D\equiv rv-su>0$ so that $f(\alpha)$ is a monotonically increasing function and α approaches the fixed point α_∞ (if it exists in [0,1]) monotonically. When parameters r, s, u, and v satisfy certain conditions, 0 and 1 in the sequence $S_\alpha(k)$ are transformed uniquely to 0 and 1 (or 1 and 0) in the sequence $S_{\alpha'}(k)$, respectively, by transformation (2.3). In fact, case (i), if

$$(r-D)i+s(k+1)>0$$

and

$$(u-r+D)i+(v-s-D)k-r-s+u+v<0\ ,$$

then $S_\alpha(k)=0$ and 1 are transformed to $S_{\alpha'}(ui+vk)=0$ and 1, respectively; case (ii), if

$$(r+D)i+(s-D)k+r+s>0$$

and

$$(u-r-D)i+(v-s)(k+1)>0\ ,$$

then $S_\alpha(k)=0$ and 1 are transformed to $S_{\alpha'}(ui+vk-1)=1$ and 0, respectively. When a consecutive pair of 0 and 1 is transformed, a gap of either $v-1$ or $u+v-1$ units appears between transformed 0 and 1. Therefore, we can determine uniquely the sequence of 0 and 1 for α' if the gap is sufficiently small. This consideration leads to a limited choice of u and v: $(u,v)=(-2,3),(-1,2),(-1,3),(1,1),(1,2)$. It should be noted, however, that it will be possible to devise other transformations which produce larger gaps for pairs.

(i) Hyperinflation rule I. We take the transformation

$$\alpha'=\frac{1}{2-\alpha}\ . \tag{2.4}$$

This transformation maps

$$[0,\tfrac{1}{2}]\to[\tfrac{1}{2},\tfrac{2}{3}]\to[\tfrac{2}{3},\tfrac{3}{4}]\to\ldots \tag{2.5}$$

and the (left) stable fixed point is at $\alpha_\infty=1$.

Under the transformation (2.4), 0's and 1's in a sequence are transformed as follows:

$$\left[\frac{i}{k},\frac{i+1}{k+1}\right]\to\left[\frac{k}{2k-i},\frac{k+1}{2k-i+1}\right]\equiv\left[\frac{i'}{k'},\frac{i'+1}{k'+1}\right]\ , \tag{2.6}$$

$$\left[\frac{i}{k+1},\frac{i}{k}\right]\to\left[\frac{k+1}{2k-i+2},\frac{k}{2k-i}\right]\subset\left[\frac{i'}{k'+1},\frac{i'}{k'}\right]\ , \tag{2.7}$$

where $k'\equiv 2k-i$, $i'\equiv k$. Therefore, $S_\alpha(k)=0$ and 1 are transformed uniquely into $S_{\alpha'}(2k-i)=0$ and 1, respectively.

Under the transformation (2.4), pairs of 0 and 1 are transformed as follows.

00. This pair is parametrized by (k,i) and $(k+1,i)$ and possible only for $\alpha\in[0,\frac{1}{2})$. These are transformed to $(2k-i,k)$ and $(2k-i+2,k+1)$. Thus, there is a gap of one unit between the transformed two 0's. However, after at least one transformation, α is in $[\frac{1}{2},1]$, in which there are no more than two 0's in a row. Therefore the gap must be filled by 1. That is, $00\to010$.

11. This pair is characterized by (k,i) and $(k+1,i+1)$. The transformation (2.4) moves this pair to $(2k-i,k)$ and $(2k-i+1,k+1)$. There is no gap between them. Thus, $11\to11$.

01. This pair is characterized by (k,i) and $(k+1,i+1)$. There is no gap as in the pair 11, and hence $01\to01$.

10. This pair is characterized by (k,i) and $(k+1,i)$. This is transformed to 1 and 0 with one missing unit in between. This must be filled by a 1 for the same reason as for the pair 00, i.e., $10\to110$.

These rules of the pairwise transformation can be uniquely reduced to a unit wise transformation

$$0\to10,\quad 1\to1\ . \tag{2.8}$$

This is the hyperinflation rule for the elements of the sequence. Namely, sequence $S_\alpha(k)$ is transformed into sequence $S_{\alpha'}(k)$ by this inflation for any α. For example, a periodic sequence 010010010..., which corresponds to $\alpha=\frac{1}{3}$, is transformed to 101101011010110... ($\alpha=\frac{3}{5}$) by the transformation (2.8). Note that the outermost entries of a transformed pair overlap with those of the neighboring pairs.

(ii) Hyperinflation rule II. The transformation

$$\alpha'=\frac{\alpha+1}{\alpha+2}\ , \tag{2.9}$$

is another example which has a stable fixed point at the inverse golden ratio, $\alpha_\infty=\tau^{-1}$ [$=(\sqrt{5}-1)/2$], an irrational number. This maps the regions $[0,F_1/F_2]\to[F_1/F_2,F_3/F_4]\to[F_3/F_4,F_5/F_6]\to\ldots$, where F_n are the Fibonacci numbers (1,2,3,5,8,13,...,) satisfying $F_{n+1}=F_n+F_{n-1}$. We restrict our attention to $\alpha\le\tau^{-1}$.

Under the transformation (2.9), we find

$$\left[\frac{i}{k},\frac{i+1}{k+1}\right]\rightarrow\left[\frac{k+i}{2k+i},\frac{k+i+2}{2k+i+3}\right]\subset\left[\frac{i'}{k'+1},\frac{i'}{k'}\right], \tag{2.10}$$

$$\left[\frac{i}{k+1},\frac{i}{k}\right]\rightarrow\left[\frac{k+i+1}{2k+i+2},\frac{k+i}{2k+i}\right]\subset\left[\frac{i''}{k'},\frac{i''+1}{k'+1}\right], \tag{2.11}$$

where

$$k'\equiv 2k+i-1,\quad i'\equiv k+i,\quad i''\equiv k+i-1\ . \tag{2.12}$$

Note that in contrast to the previous case, we have chosen to transform 0 to 1 and 1 to 0.[10] Therefore a region 0 with (k,i) in the sequence (2.1) can be transformed into a region of 1 with $(k',i')\equiv(2k+i-1,k+i)$. Similarly, a region of 1 with (k,i) is transformed into a region of 0 with $(k',i'')\equiv(2k+i-1,k+i-1)$. Using the fact that (i) for $\alpha\leq\tau^{-1}<\frac{2}{3}$ no 111's are possible and that (ii) after one transformation of (2.9), $\alpha\geq\frac{1}{2}$, where there are no 00's, we find the following transformation for the pairs:

$$00\rightarrow 101,\ 11\rightarrow 0110,\ 01\rightarrow 1010,\ 10\rightarrow 011\ . \tag{2.13}$$

Furthermore, transformation (2.13) is reducible to

$$0\rightarrow 10,\ 1\rightarrow 101\ . \tag{2.14}$$

It is interesting to note the fact that transformation (2.9) is obtained by applying the transformation $\alpha'=1/(\alpha+1)$ twice, and the inflation rule (2.14) is a square transformation of $0\rightarrow 1, 1\rightarrow 10$, which is the inflation rule for the Fibonacci chain.

(iii) Hyperinflation rule III. As a next example, we consider the transformation

$$\alpha'=\frac{\alpha}{\alpha+1}\ . \tag{2.15}$$

This transforms $[\frac{1}{2},1]\rightarrow[\frac{1}{3},\frac{1}{5}]\rightarrow\ldots$ and has a fixed point at $\alpha_\infty=0$. Under the transformation (2.15), the region 0 in Eq. (2.1) can be transformed into a region of 0 with $(k',i')\equiv(k+i,i)$ and the region of 1 is transformed into a region of 0 with $(k',i')\equiv(k+i,i)$. It is easy to show the pairs of 00, 01, 10, 11 are transformed to 00, 001, 10, 0101, respectively. Thus, the transformation (2.15) corresponds to hyperinflation $0\rightarrow 0$ and $1\rightarrow 01$ in the sequence.

Other transformations we can easily find are $\alpha'=1/(3-\alpha)$ which transforms $0\rightarrow 01$ and $1\rightarrow 010$ and has a fixed point at $1-\tau^{-1}$ (this can be viewed as the complement of the hyperinflation rule II), and repeated transformation of rule I $[\alpha'=(2-\alpha)/(3-2\alpha);0\rightarrow 110, 1\rightarrow 1]$ and rule III $[\alpha'=\alpha/(2\alpha+1);0\rightarrow 0, 1\rightarrow 001]$.

III. DIFFRACTION PATTERN

The diffraction intensity $I(k,\alpha)$ from the lattice (1.1) is determined by the absolute square of the Fourier transformation $F(k,\alpha)$ of the density function of the lattice points

$$F(k,\alpha)=\sum_n \exp(ikx_n)\ . \tag{3.1}$$

We first calculated the Fourier sum (3.1) numerically. Figure 1 shows the diffraction pattern in the (k,α) plane when (a) $\rho=1$ and (b) $\rho=\alpha$, where a dot represents the point at which the intensity $I(k,\alpha)$ exceeds a cutoff Λ. In this figure, the sum was evaluated for 100 lattice points and Λ was set to 0.001. The diffraction intensity becomes infinity at the reciprocal-lattice points if the system is infinitely large and the apparent width of the lines is due to the finiteness of the system size. The points at $\alpha=0$ and $\alpha=1$ are the reciprocal-lattice points of the chain consisting of pure $a_0=1$ and $a_1=1+\rho$, respectively, and points at $\alpha=0.5$ are the reciprocal-lattice points for the chain of $(a_1a_0)^n$, and so forth. For $0<\alpha<1$, we see a self-similar structure with apparent wide gaps at simple rational numbers. As we will show below, this self-similarity is a consequence of the hyperinflation symmetry.

For $\alpha=m/(m+1)$ $(m=0,1,2,\ldots,)$, the chain is periodic $(a_1^m a_0)^n$. Thus the Fourier transform $F(k)$ is given by the product of the Laue function $\mathcal{L}(k)$ and the structure factor $\mathcal{S}(k)$, where

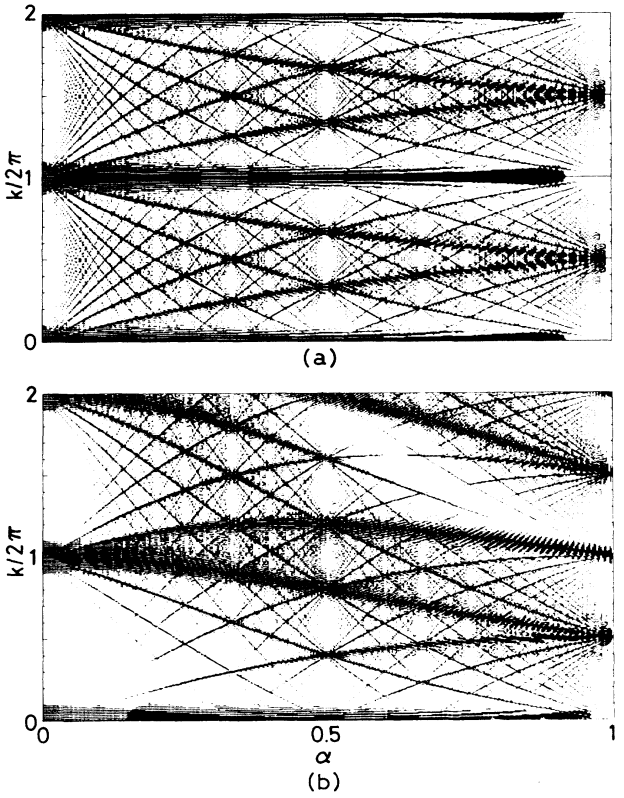

FIG. 1. Diffraction pattern from one-dimensional lattice: (a) $x_k=[\alpha k]$, (b) $x_k=\alpha[\alpha k]$. Dots represent points where the scattering intensity from 100 lattice points exceeds a cutoff $\Lambda=0.001$. Namely dots are the reciprocal-lattice points. The structure of the reciprocal-lattice points becomes very simple for simple rational numbers.

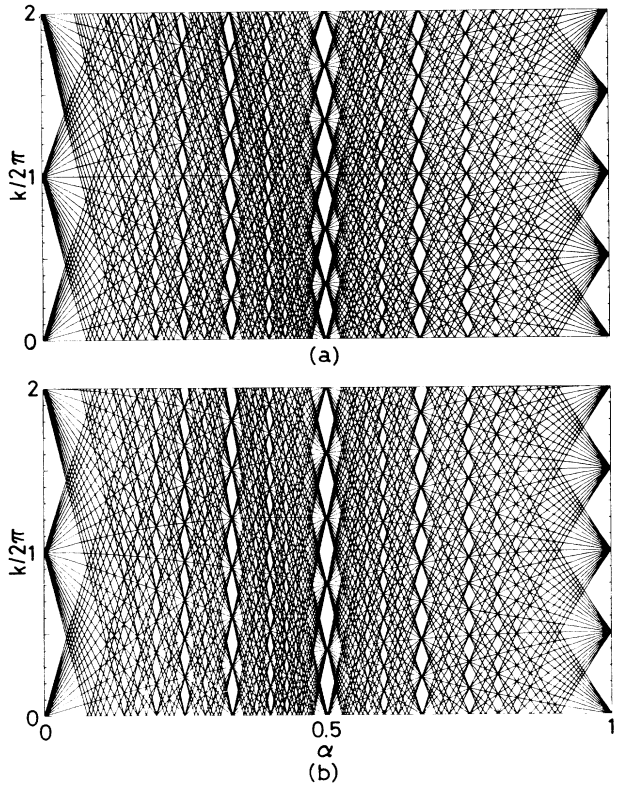

FIG. 2. Loci of the reciprocal-lattice point: (a) $x_k=[\alpha k]$, (b) $x_k=\alpha[\alpha k]$. Agreement with Fig. 1 is excellent.

$$\mathcal{L}(k)=\sum_J \exp(ik_m J)\propto \sin(k_m N/2)/\sin(k_m/2) \tag{3.2}$$

with $k_m=k(ma_1+a_0)$ and

$$\mathcal{S}(k)=\sum_j^m \exp(ika_1 j)\propto U_m(\cos(ka_1/2)) \ . \tag{3.3}$$

Here, $U_m(\cos\theta)\equiv\sin[(m+1)\theta]/\sin\theta$ is the Tchebycheff polynomial of the second kind and N is the number of the unit cells in the system. When N increases, the Laue function approaches to a set of δ functions at reciprocal-lattice points $K_n=2\pi n/(ma_1+a_0)$, n being an integer. Apparent lines in Fig. 1 are the loci of the reciprocal-lattice points. In fact the loci of these points are given by

$$k(\alpha,p,q)=2\pi\frac{(1-\alpha)p+\alpha q}{\rho\alpha+1} \ , \tag{3.4}$$

where p and q are integers. Figure 2 shows some of loci determined by Eq. (3.4) which are identical to those in Fig. 1. The locus $k(\alpha,p,q)$ approaches $2\pi p$ as α approaches zero and $2\pi q/(1+\rho)$ as α approaches unity. These are the reciprocal-lattice points of the regular chain of a_0 $(=1)$ and a_1 $(=1+\rho)$, respectively. Therefore, the loci are the smooth interpolation of these reciprocal-lattice points which pass the reciprocal-lattice points of regular chains. Furthermore, the diffraction pattern obtained for the quasiperiodic lattices with irrational α's consists of δ functions at points given by Eq. (3.4).[3,11] Thus the loci (3.4) determine the reciprocal-lattice points for any value of α. Note that we can proceed in the same way as above for $\alpha=1/(m+1)$ and find that the loci of the reciprocal-lattice points for $\alpha=1/(m+1)$ are given by Eq. (3.4).

The structure factor at K_n can be calculated straightforwardly as

$$\mathcal{S}(k_n)\propto \sin\frac{(a_1-a_0)n\pi}{ma_1+a_0}\Big/\sin\frac{a_1 n\pi}{ma_1+a_0} \ . \tag{3.5}$$

Therefore, the structure factor vanishes when a_1 and a_0 satisfy a certain condition. For example, when $m=1$, i.e., $\alpha=0.5$, the reciprocal-lattice points are given by $K_n=2n\pi/(a_1+a_0)$ and the structure factor becomes $\mathcal{S}(K_n)\propto\cos[na_1\pi/(a_1+a_0)]$. This structure factor vanishes, for example, for $n=2\times$(odd integer) when $a_1=3a_0$. Since the structure factor may vanish only when a_1 and a_0 satisfy a certain condition, it is rather atypical for arbitrary spacings and we do not argue this possibility any further.

We can derive the transformation of the diffraction pattern, noting that $\alpha=m/(m+1)$ obeys the hyperinflation transformation I. First, we pick up one of the reciprocal-lattice points at $\alpha=1$; $k=2\pi q/(1+\rho)$. Then, we associate an integer p and a real number z to any point in the (α,k) plane by

$$k(\alpha)=2\pi\frac{(1-\alpha)(p+z)+\alpha q}{\rho\alpha+1} \ , \tag{3.6}$$

keeping q fixed. We identify the transformation of the point under the hyperinflation $\alpha'=1/(2-\alpha)$ by

$$k(\alpha')=2\pi\frac{(1-\alpha')(p+z)+\alpha' q}{\rho\alpha'+1} \ . \tag{3.7}$$

(Note when ρ is taken to be α, we have to change ρ in these equations accordingly.) Eliminating $p+z$ from these equations, we obtain the following transformations:

$$k(\alpha')\equiv k'=\frac{(1+\rho\alpha)k+2\pi(1-\alpha)q}{\rho+2-\alpha} \tag{3.8}$$

when ρ is a constant and

$$k(\alpha')\equiv k'=\frac{(2-\alpha)[(1+\alpha^2)k+2\pi(1-\alpha)q]}{\alpha^2-4\alpha+5} \tag{3.9}$$

when $\rho=\alpha$. Figure 3 shows the hyperinflation of the region $\alpha\in[0.5,1]$ in Fig. 1 to [0,1] by Eqs. (3.8) and (3.9) with $q=0$. The apparent width of each line is again due to the finiteness of the lattice points. It is evident from Fig. 3 that the self-similarity holds exactly. It is easy to show that the function (3.4) is invariant under the hyperinflation transformation (2.4) and (3.8) [or (3.9)] independent of the choice of q.

IV. PROPERTIES OF SYSTEMS DESCRIBED BY $SL(2,C)$

A. General consideration

As we summarize in the Appendix, many physical systems in one dimension can be described in terms of 2×2

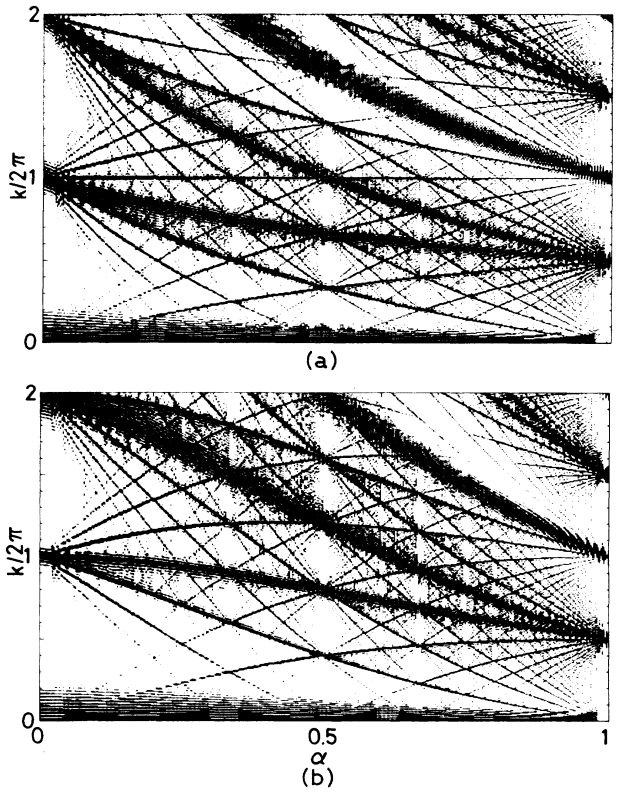

FIG. 3. Similarity transformation of the diffraction pattern: (a) transformation (3.8) for $x_k=[\alpha k]$, (b) transformation (3.9) for $x_k=\alpha[\alpha k]$. In both figures, q is set to zero and $\alpha\in[0.5,1]$ in Fig. 1 is inflated to [0,1].

unimodular transfer matrices. Various properties of the whole system are determined by the infinite product of the transfer matrices $SL(2,C)$.[12,13] Namely, denoting the $SL(2,C)$ element for the jth unit by g_j, physical quantities, two-vectors $\{v_j\}$, or complex numbers $\{z_j\}$, are transformed by

$$v_j=g_j v_{j-1}$$

or (4.1)

$$z_j=g_j\circ z_{j-1}\equiv\frac{g_{11}(j)z_{j-1}+g_{12}(j)}{g_{21}(j)z_{j-1}+g_{22}(j)}\ ,$$

where

$$g_j\equiv\begin{bmatrix}g_{11}(j) & g_{12}(j)\\ g_{21}(j) & g_{22}(j)\end{bmatrix}\ , \tag{4.2}$$

and $\det g_j=1$. The physical properties of the total system are related to the matrix elements of

$$g\equiv g_N\cdots g_1\equiv\begin{bmatrix}g_{11} & g_{12}\\ g_{21} & g_{22}\end{bmatrix}\ , \tag{4.3}$$

as is described in the Appendix. Physical properties show totally different behavior as a function of the parameters in $\{g_j\}$, according to the divergence or convergence of the product. For example, a product of random g_j is known to cause localization of wave propagating in the chain,[14] and a regular product of g_j determines the energy bands for a regular chain. For any sequence of g_j, there exists critical values of the parameters in g_j which determine the boundary of two different physical situations such as transparent and opaque, and allowed and forbidden energy band.

We consider a chain consisting of two $SL(2,C)$'s, g_0 and g_1 in the order of $S_\alpha(k)$ of Eq. (2.1) and examine the convergence of their ordered N product

$$g\equiv\prod_{k=1}^{N}g_{S_\alpha(k)}=g_{S_\alpha(N)}\cdots g_{S_\alpha(1)}\ . \tag{4.4}$$

Two sequences related by a hyperinflation must show self-similar properties under the corresponding transformation of g_0 and g_1. For example, under the hyperinflation rule II the transformation becomes

$$g_0'=g_1g_0,\quad g_1'=g_1g_0g_1\ , \tag{4.5}$$

which is taken, in general, in the six-dimensional parameter space.

The asymptotic property of g can be easily analyzed when α is rational, in particular when $\alpha=m/(m+1)$ and $\alpha=1/(m+1)$ where the system becomes a periodic chain of $g_0g_1^m$ or $g_0^mg_1$. First, we can show easily for any unimodular matrix

$$A=\begin{bmatrix}a_{11} & a_{12}\\ a_{21} & a_{22}\end{bmatrix}\quad(\det A=1)$$

that A^m is given by

$$A^m=\begin{bmatrix}a_{11}U_{m-1}-U_{m-2} & a_{12}U_{m-1}\\ a_{21}U_{m-1} & a_{22}U_{m-1}-U_{m-2}\end{bmatrix}\ , \tag{4.6}$$

where $U_m\equiv U_m(\cos\theta)=\sin[(m+1)\theta]/\sin\theta$ is the Tchebycheff polynomial of the second kind defined in Sec. III and $\mathrm{tr}\,A=2\cos\theta$. (When $\mathrm{tr}\,A>2$, the analytic continuation must be used.) Therefore, the critical point for $\alpha=m/(m+1)$ which differentiates convergence and divergence of the product is given by

$$|\mathrm{tr}(g_0g_1)U_{m-1}(\mathrm{tr}g_1/2)-\mathrm{tr}g_0U_{m-2}(\mathrm{tr}g_1/2)|=2\ . \tag{4.7}$$

In general, the critical points are in seven-dimensional space (α and six parameters of the two unimodular matrices). To simplify the presentation and analysis, we survey three typical cases using prototype matrices and investigate them in the lower dimensional subspace. Application to individual problems is straightforward.

B. Numerical analysis

Numerical analysis was carried out for the product of 500 matrices. We examined the regions in the parameter space where any element of the product matrix exceeds a cutoff Λ at any point of the multiplication.

(i) Schrödinger equation-type matrices.

$$g_1=\begin{bmatrix}a & -1\\ 1 & 0\end{bmatrix},\quad g_0=\begin{bmatrix}b & -1\\ 1 & 0\end{bmatrix}\ . \tag{4.8}$$

This type of matrix applies to a tightly bound electron

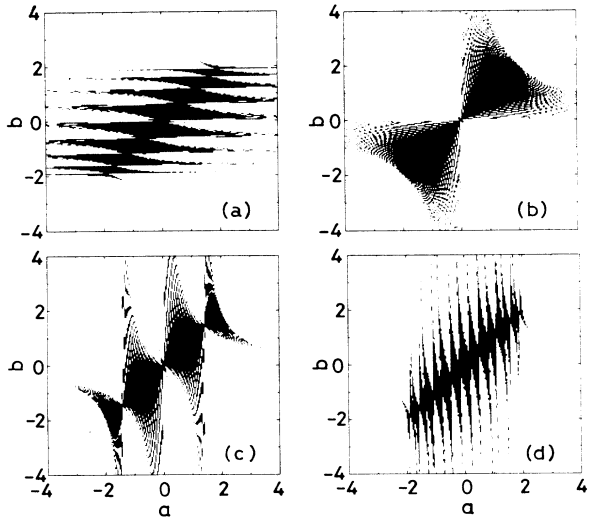

FIG. 4. Convergent regions for the Schrödinger equation-type matrix for various values of α in the (a,b) plane: (a) $\alpha=\frac{197}{1987}$, (b) $\alpha=\frac{977}{1987}$, (c) $\alpha=\frac{1499}{1987}$, (d) $\alpha=\frac{1777}{1987}$. The product of $N=500$ matrices is considered to be divergent if (1,1) or (2,2) matrix element exceeds the cutoff $\Lambda=10^2$ during the multiplication in Eq. (4.4).

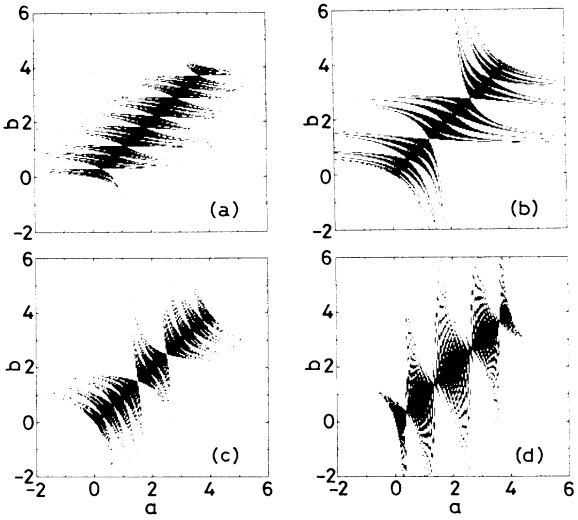

FIG. 6. Convergent regions for the lens-type matrix for various values of α in the (a,b) plane: (a) $\alpha=\frac{397}{1987}$, (b) $\alpha=\frac{797}{1987}$, (c) $\alpha=\frac{1193}{1987}$, (d) $\alpha=\frac{1597}{1987}$. The product of $N=1000$ matrices is considered to be divergent if (2,1) matrix element exceeds the cutoff $\Lambda=10^2$ during the multiplication in Eq. (4.4).

with modulation in the site energy $[a(b)=E-\varepsilon_{a(b)}]$ and to lattice vibration with modulation in the mass $[a(b)=2-m_{a(b)}\omega^2]$ (see Appendixes A and C). The relevant parameter space is three dimensions (α,a,b) and intersections in the (a,b) plane at various α's and in the (α,b) plane at various a's are shown in Figs. 4 and 5, respectively. One can see in Fig. 4 how the convergent region $|b|\leq 2$ at $\alpha=0$ deforms itself towards those $|a|\leq 2$ at $\alpha=1$ via $0\leq ab\leq 2$ at $\alpha=0.5$. Note that the line $a=b$ between (2,2) and $(-2,-2)$ is fixed.

(ii) Lens-type matrices.

$$g_1=\begin{bmatrix}1-a & -1\\ a & 1\end{bmatrix},\quad g_0=\begin{bmatrix}1-b & -1\\ b & 1\end{bmatrix}. \tag{4.9}$$

The parameters a and b can be considered as the inverse of the focal length of two lenses (see Appendix E). Figures 6 and 7 show the convergent region of the product in the (a,b) plane and in the (α,b) plane, respectively. The line $a=b$ between (0,0) and (4,4) is fixed.

(iii) Kronnig-Penny-type matrices.

$$g_1=\begin{bmatrix}1-ia & -iaZ_j^*\\ iaZ_j & 1+ia\end{bmatrix},\qquad g_0=\begin{bmatrix}1-ib & -ibZ_j^*\\ ibZ_j & 1+ib\end{bmatrix}, \tag{4.10}$$

where $Z_j=\exp(2ikz_j)$ and z_j denotes the position of the

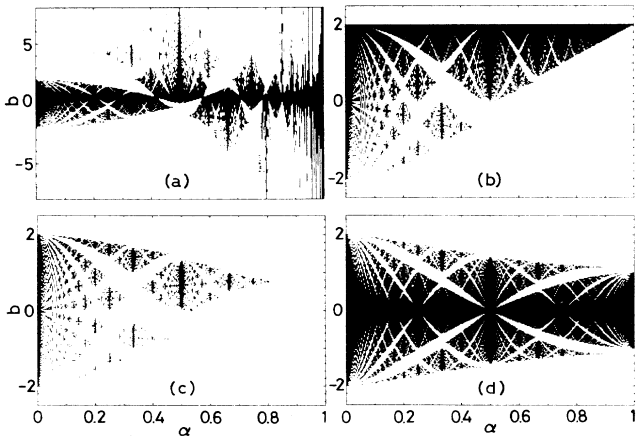

FIG. 5. Convergent regions for the Schrödinger equation-type matrix in the (α,b) plane: (a) $a=0.5$, (b) $a=2.0$, (c) $a=3.0$, (d) $a=b$. The criterion for the convergence is $\Lambda=10^3$ for the product of 500 matrices. Note the change in scale in (a).

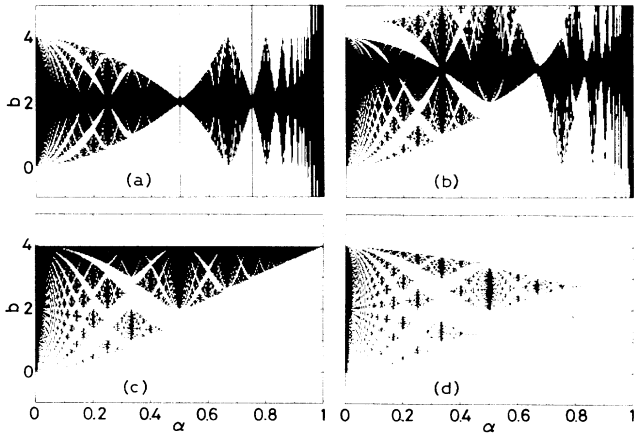

FIG. 7. Convergent regions for the lens-type matrix for various values of a in the (α,b) plane: (a) $a=2$, (b) $a=3$, (c) $a=4$, (d) $a=5$. The convergence criterion is $\Lambda=10^4$ for the product of 500 matrices.

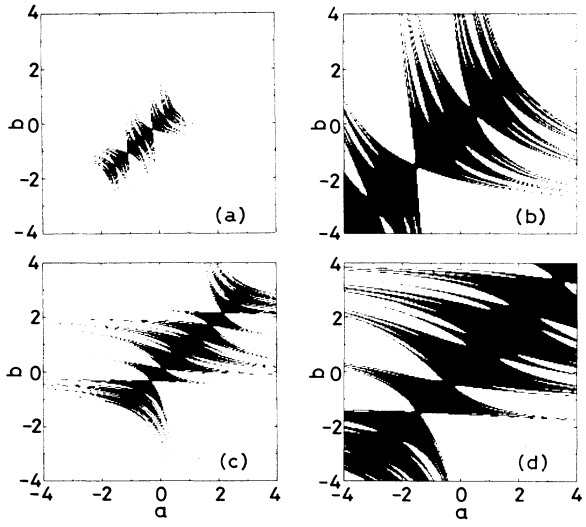

FIG. 8. Convergent regions for the Kronig-Penny–type matrix for various values of α in the (a,b) plane: (a) $\alpha=\tau^{-1}$ and $k=1$, (b) $\alpha=\tau^{-1}$ and $k=4$, (c) $\alpha=\tau^{-1}/2$, and $k=2$, (d) $\alpha=\tau^{-1}/2$ and $k=5$. The product of $N=500$ matrices is considered to be divergent if (2,2) matrix element exceeds the cutoff $\Lambda=10^2$ during the multiplication in Eq. (4.4).

jth potential placed periodically with unit spacing. The parameters a and b are in proportion to the strength of the δ potential (see the Appendix). The convergent regions of the product shown in Figs. 8 and 9 are the allowed region, i.e., the energy band. One can see how the energy bands for $\alpha=0$ and 1 are interpolated as α moves between these two limits.

As can be seen in these figures, the qualitative behavior is the same for these models. Other types of matrices also show similar structures. The apparent multilevel branch structure is explained by the hyperinflation symmetry in the chain.

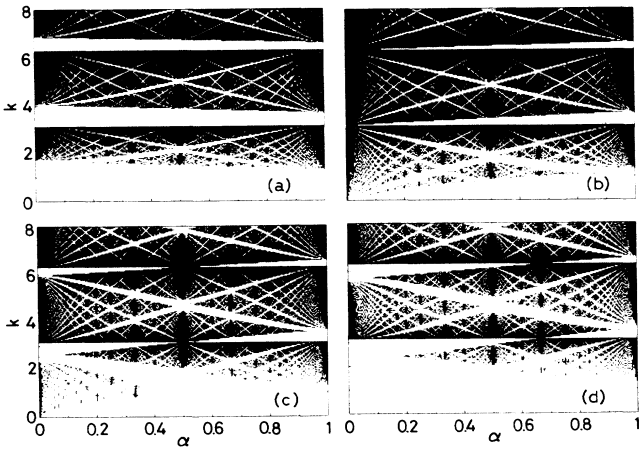

FIG. 9. Convergent regions for the Kronig-Penny–type matrix for various values of a,b in the (α,k) plane: (a) $a=1$ and $b=2$, (b) $a=1$ and $b=0$, (c) $a=1$ and $b=-1$, (d) $a=1$ and $b=-2$. The convergence criterion is the same as in Fig. 8.

C. Analysis for some rational α's

Taking the Schrödinger equation-type matrices as an example, we analyze the self-similar structure of the convergent regions. Setting $\mathrm{tr}g_1=a$, $\mathrm{tr}g_0=b$, and $\mathrm{tr}g_0g_1=ab-2$, we obtain the condition for the critical points for $\alpha=m/(m+1)$,

$$|bU_m(a/2)-2U_{m-1}(a/2)|=2 \ . \tag{4.11}$$

Therefore, the critical points for a given a at $\alpha=m/(m+1)$, $b_m^{(\pm)}$, are given by

$$b_m^{(\pm)}=\frac{2[U_{m-1}(a/2)\pm 1]}{U_m(a/2)} = \begin{cases} 2\cos[(m-1)\theta/2]/\cos[(m+1)\theta/2] \\ 2\sin[(m-1)\theta/2]/\sin[(m+1)\theta/2] \end{cases}$$

with $a=2\cos\theta$ when $a\le 2$. (When $a>2$, $a=2\cosh\theta$ and cos and sin must be read as cosh and sinh.) The loci of these critical points for $a>2$ are written as

$$b^{+}(\alpha)=\frac{2\cosh\left[\left(\frac{2\alpha-1}{1-\alpha}\right)\frac{\theta}{2}\right]}{\cosh\left[\left(\frac{1}{1-\alpha}\right)\frac{\theta}{2}\right]}$$

and (4.12)

$$b^{-}(\alpha)=\frac{2\sinh\left[\left(\frac{2\alpha-1}{1-\alpha}\right)\frac{\theta}{2}\right]}{\sinh\left[\left(\frac{1}{1-\alpha}\right)\frac{\theta}{2}\right]} \ .$$

The critical points $b^{(\pm)\prime}(\alpha')$ at $\alpha'=1/(2-\alpha)$ and $b^{\pm}(\alpha)$ can be shown to satisfy the following relation:

$$b^{(\pm)\prime}=\frac{2(b^{(\pm)}+2)}{-b^{(\pm)}+2a+2} \ . \tag{4.13}$$

Thus we can consider the transformation

$$b'=\frac{2(b+2)}{-b+2a+2} \tag{4.14}$$

as an approximate similarity transformation in the (α,b) subspace for the hyperinflation rule $\alpha'=1/(2-\alpha)$. In fact, we can see from Fig. 2 in Ref. 5 that this transformation is an excellent approximation.

We can also calculate critical points for $\alpha=1/(m+1)$ from Eq. (4.11), noting that the convergence criteria for g is invariant under the transformation $\alpha\to 1-\alpha$ and $0\to 1$ and $1\to 0$. Using the definition of the Tchebycheff polynomial, we can rewrite the condition (4.11) as

$$\sin[(m+1)\theta/2]\{a\cos[(m+1)\theta/2] -2\cos[(m-1)\theta/2)]\}=0 \tag{4.15}$$

and

$$\cos[(m+1)\theta/2]\{a\sin[(m+1)\theta/2] -2\sin[(m-1)\theta/2)]\}=0 \ , \tag{4.16}$$

where $b=2\cos\theta$. Therefore, $b=2\cos[p\pi/(m+1)]$ $(p=1,2,3,\ldots,m)$ are the critical points independent of the value of a. Note these points are nothing but the Tchebycheff points of the second kind (times 2). The loci of these points are given by

$$b=2\cos(j\alpha\pi),\quad b=2\cos[(1-j\alpha)\pi] \tag{4.17}$$

for $\alpha\le 1/(j+1)$ $(j\in\mathcal{N})$.

Other critical points for $\alpha=1/(m+1)$ are determined by the implicit equations

$$\tan(m\theta/2)\tan(\theta/2)=(a-2)/(a+2) \tag{4.18}$$

and

$$\tan(m\theta/2)\cot(\theta/2)=(2+a)/(2-a) \tag{4.19}$$

when $|b\equiv 2\cos\theta|\le 2$. When $|b|>2$, the analytic continuation must be taken with $b=2\,\mathrm{sign}(b)\cosh\theta$ and a being changed to $-a$, and the right-hand side of the first equation is multiplied by -1. The loci of these boundaries are given as follows.

(i) When $|b|\le 2$,

$$\frac{1-\alpha}{\alpha}=\begin{cases}2(\Theta_+ +p\pi)/\theta\ ,\\ 2(\Theta_- +p\pi)/\theta\ ,\\ 2[\Theta_+ -(p+1/2)\pi]/(\theta-\pi)\ ,\\ 2[\Theta_+ -p\pi]/(\Theta-\pi)\ ,\end{cases} \tag{4.20}$$

if $0\le a<2$, where

$$\Theta_\pm=\tan^{-1}[\pm(2\pm a)/(2\mp a)\sqrt{(2\mp b)/(2\pm b)}]$$

and $\theta=\cos^{-1}(b/2)$. For $a>2$, Θ_+ and Θ_- must be interchanged in Eq. (4.20).

(ii) When $b>2$ and $|a|\le 2$,

$$\frac{1-\alpha}{\alpha}=\frac{2\tanh^{-1}\left[\dfrac{2\pm a}{2\mp a}\left[\dfrac{b\mp 2}{b\pm 2}\right]^{1/2}\right]}{\cosh^{-1}(b/2)}\ . \tag{4.21}$$

(iii) When $b<-2$ and $|a|\le 2$,

$$\frac{1-\alpha}{\alpha}=\frac{2\tanh^{-1}\left[\dfrac{2\pm a}{2\mp a}\left[\dfrac{b\pm 2}{b\mp 2}\right]^{1/2}\right]}{\cosh^{-1}(-b/2)}\ . \tag{4.22}$$

There are no boundaries when $|b|>2$ and $|a|>2$. Some of the loci (4.17) and (4.20) are shown in Fig. 10 for $a=3.0$ and $0\le\alpha\le 0.5$. The agreement with Fig. 5(c) is excellent.

We can also find an approximate similarity transformation based on the hyperinflation rule III in the (α,b) plane. We first find a parameter j associated with a given point in the (α,b) plane such that

$$C(j+1,\alpha)<b\le C(j,\alpha)\ , \tag{4.23}$$

where $C(j+1,\alpha)\equiv 2\cos(j\alpha\pi)$, that is,

$$j=[\arccos(b/2)/\alpha\pi]\ . \tag{4.24}$$

Keeping the same relative position within the neighboring loci, we take

$$b'=\frac{[C(j+1,\alpha')-C(j,\alpha')]b+C(j+1,\alpha)C(j,\alpha')-C(j+1,\alpha')C(j,\alpha)}{C(j+1,\alpha)-C(j,\alpha)} \tag{4.25}$$

as an approximate transformation for $\alpha'=\alpha/(\alpha+1)$. Figure 11 shows the hyperinflation by Eq. (4.25) of the region $\alpha\in[0,\frac{1}{3}]$ to $[0,\frac{1}{2}]$.

We can analyze other series of α in the same fashion and derive the deeper structure of the convergent regions.[1] As an example, we consider the case $a=2b$ shown in Fig. 5(d). We find that the boundary point between convergent and divergent regions is determined by

$$U_{2m+1}(\cos\theta)-2U_{2m-1}(\cos\theta)=2\sqrt{2}$$

for $\alpha=m/(2m+1)$ which converges to 0.5 from below as $m\to\infty$ and by

$$2U_{2m+1}(\cos\theta)-U_{2m-1}(\cos\theta)=2\sqrt{2}$$

for $\alpha=(m+1)/(2m+1)$ which converges to 0.5 from above as $m\to\infty$, where $a=2b=2\sqrt{2}\cos\theta$.

D. Isolated points

In Figs. 4–9, we see isolated points converging outside of the boundaries determined above. (These points are identical to energy levels due to an isolated impurity in binary alloys.) This kind of isolated levels can be calculated by looking at the matrix of the type g_iX^∞ or $X^\infty g_i$ $(i=0,1)$, where X is a unit repeated in the sequence for rational α's. Let us assume that in a representation which diagonalizes X,

$$X=\begin{bmatrix}\lambda_+ & 0\\ 0 & \lambda_-\end{bmatrix},\quad g_1=\begin{bmatrix}g'_{11} & g'_{12}\\ g'_{21} & g'_{22}\end{bmatrix}, \tag{4.26}$$

where $\lambda_+>1$. Then g_1X^∞ has vanishing trace, corresponding to a convergent product of the transfer matrices, only when $g'_{11}=0$. This determines the isolated

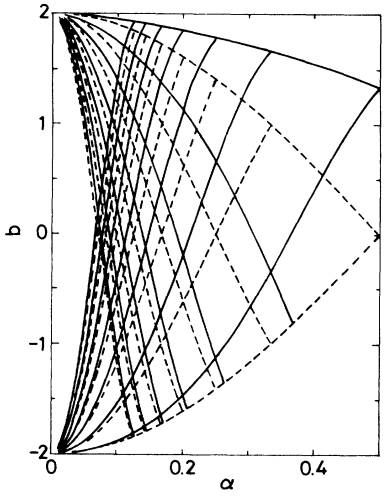

FIG. 10. Loci determined by Eq. (4.17) (dashed lines) and Eq. (4.20) (solid lines). Seven loci are shown for $\alpha=3.0$. These loci determine the first-order complexity of the structure for $\alpha\in[0,0.5]$ seen in Fig. 5(c). The deeper levels are determined by other series of rational numbers.

level. For example, when $\alpha\sim 0$, we take $X=g_0$ and find an isolated level at $b=a/2+2/a$ [or $a=b-(b^2-4)^{1/2}$].

We have analyzed the series $\alpha=1/(m+1)$ in this manner taking $X=g_1 g_0^m$ and have found that some of the isolated levels are determined by the following equation:

$$[2b-a+\sqrt{\Delta(a,b)}][a+\sqrt{\Delta(a,b)}]=1 , \tag{4.27}$$

where $\Delta(a,b)=[(au_m-2u_{m-1})^2-4]/4u_m^2$ and $u_m=U_m(b/2)$. As an example, we consider again the case $a=2b$ shown in Fig. 5(d). For this case, Eq. (4.27) is simplified to

$$(2b+\sqrt{\Delta})\sqrt{\Delta}=1 ,$$

where $\Delta\equiv\Delta(2b,b)=(u_m^2-1)/u_{m-1}^2$. For $m\to\infty$, i.e., $\alpha\to 0$, the smallest positive solution of this equation is given by

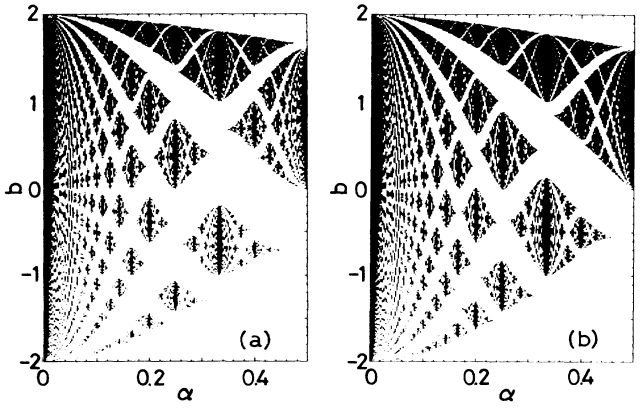

FIG. 11. Similarity transformation of the convergent region for the Schrödinger equation-type matrix by Eq. (4.25) for $a=2.5$. $\alpha\in[0,\frac{1}{3}]$ is transformed to [0,0.5] in (b) via Eq. (4.25), which can be compared with (a) before the transformation. ($N=500$, $\Lambda=10^2$.)

$$\theta=\frac{\pi}{m+1}\left[1-\frac{\sqrt{2}+1}{m+1}+O(m^{-2})\right] . \tag{4.28}$$

On the other hand, the small critical θ, that is the upper boundary of the continuum determined by Eqs. (4.15) and (4.16) is given by

$$\theta=\frac{\pi}{m+2}=\frac{\pi}{m+1}\left[1-\frac{2}{m+1}+O(m^{-2})\right] . \tag{4.29}$$

Thus the gap between the edge of the continuum and the isolated level is of $O(m^{-2})$ and approaches zero quickly as $\alpha\to 0$.

V. DISCUSSION

In this paper, we have presented the hyperinflation rules in periodic and quasiperiodic sequences given by Eq. (2.1), analysis of the diffraction pattern and physical properties determined by $SL(2,C)$. It is considered rather peculiar that physical properties show completely different nature depending on the rationality and irrationality of a parameter.[1] We have demonstrated that various physical properties show self-similarity as a function of this parameter because of the hyperinflation rule. The diffraction pattern has been shown to obey a similarity transformation determined by the loci of the reciprocal-lattice vectors, including quasiperiodic systems. Figure 3 also implies that the Brillouin zones of one-dimensional chains are self-similar and hence the energy band will show self-similarity.

We have also obtained transformations (4.14) and (4.25) for the self-similar structure of the convergent region of g matrix for the Schrödinger equation-type system. These transformations are approximations, since, as we mentioned in Sec. IV, the hyperinflation transformation transforms parameters in the seven-dimensional space determined by Eq. (4.5). Despite of this fact the transformation seems very accurate as one can see in Fig. 11.

The self-similar structure was analyzed in this paper by tracing critical points along certain series of rational numbers. We can analyze the structure at deeper level by following other series of rational α (Ref. 1) as we have shown at the end of Sec. IV C. We can go down to deeper and deeper level and we will see similar structure at any level.

It is straightforward to apply present results to individual physical systems. For example, the energy (and gap) spectra of binary system with site energy ε_0 and ε_1 for the tightly bound electron can be obtained by taking the subspace $b-\varepsilon_0=a-\varepsilon_1$ in the (α,a,b) space in Fig. 4. Namely the intersection of this line in Fig. 4 gives the energy spectra studied by many authors.[15,16] Transmission of light through optical layers,[17] energy band of the Kronig-Penny model, hopping conduction[18] are among other systems. Recently, quasiperiodic superlattices have been fabricated[5] and we expect to see various physical properties self-similar as a function of α, though the precise control of thickness of layers might be very difficult. As we explain in the Appendix, a set of lenses and a set of two-port circuits are also described by an $SL(2,C)$ for-

malism which can be studied easily. We thus propose experimental observation of the present results by these rather simple experiments. For a set of lenses, we expect to see the self-similar structure in the effective focal length as a function of α. The two-port circuit will also show self-similarity in its effective impedance as a function of α.

We have restricted our discussion in this paper to semi-infinite sequences generated by Eq. (2.1) with positive integers k. We can construct infinite sequences by allowing $k \leq 0$. It is straightforward to show that the hyperinflation rules hold for the negative side of the sequence.

We have found three essentially different hyperinflation transformations whose fixed points are 0,1, and the inverse golden ratio. There will be other hyperinflation rules whose fixed point is different from those studied here. We have not yet been able to exhaust and classify all of the possible hyperinflation rules and this is still an open question.

ACKNOWLEDGMENT

The work of H.A. was supported in part by National Science Foundation Grant No. PHY-87-06873.

APPENDIX

In this appendix we summarize transfer matrix formalism of various one-dimensional systems. The product of N matrices is written as

$$g_N \cdots g_1 \equiv \begin{bmatrix} g_{11} & g_{12} \\ g_{21} & g_{22} \end{bmatrix} . \tag{A1}$$

A. Tightly bound electrons

We consider the stationary Schrödinger equation

$$Ea_j = \varepsilon_j a_j + t_{j-1} a_{j-1} + t_j a_{j+1} , \tag{A2}$$

where a_j is the probability amplitude of an electron at site j, ε_j is the site energy of site j, and t_j is the nearest-neighbor transfer energy between sites j and $j+1$. We assume that t_j is real. The Schrödinger equation can be written in the form (4.1), for

$$v_j \equiv \sqrt{t_j} \begin{bmatrix} a_{j+1} \\ a_j \end{bmatrix} ,$$
$$g_j = \left[\frac{t_j}{t_{j-1}} \right]^{1/2} \begin{bmatrix} \dfrac{E-\varepsilon_j}{t_j} & -\dfrac{t_j - 1}{t_j} \\ 1 & 0 \end{bmatrix} . \tag{A3}$$

To find the transmission coefficient, we embed an N segment in an infinite regular chain and consider the transmission of a wave incident from the left with unit amplitude

$$a_j = \begin{cases} z^j + r z^{*j}, & j = 1, 0, -1, -2, \ldots , \\ t z^j, & j = N, N+1, N+2, \ldots , \end{cases} \tag{A4}$$

where $z = e^{ika}$ and a is the lattice constant. The coefficient t gives the transmission coefficient, and r the reflection coefficient. We assumed that t_0 and t_N are the free value, say, 1. One can easily find[13]

$$r = -\frac{g_{11} z + g_{12} - g_{21} z^2 - g_{22} z}{g_{11} z^* + g_{12} - g_{21} |z|^2 - g_{22} z} ,$$
$$t = \frac{z - z^*}{g_{11} z^* + g_{12} - g_{21} |z|^2 - g_{22} z} . \tag{A5}$$

The conductivity of the chain can be obtained from the transmission coefficient using the Landauer formula.[19]

B. Potential barriers (Ref. 20)

We consider the transmission of a quantum wave through a set of potential barriers (or wells). The potential barriers are equally spaced and have the same shape of symmetric rectangular. The center of each barrier is at $z_j = (2j-1)a/2$, $j = 1, N$ and the height and width of each barrier are ϕ_j and w_j. We assume $w_j < a$ for all j so that there is always a free space between neighboring potential barriers.

Now write the quantum wave in the free space between jth and $(j+1)$st barriers as $t_j e^{ikx} + r_j e^{-ikx}$. Then we can show that Eq. (4.1) holds for

$$v_j = \begin{bmatrix} t_j \\ r_j \end{bmatrix}$$

with

$$g_j = \frac{1}{4kk_j} \begin{bmatrix} [2i(k_j^2 + k^2)s_j + 4kk_j c_j] W_j^* & 2i(k_j^2 - k^2) Z_j^* s_j \\ -2i(k_j^2 - k^2) Z_j^* s_j & [-2i(k_j^2 + k^2)s_j + 4kk_j c_j] W_j^* \end{bmatrix} , \tag{A6}$$

where $k \equiv \sqrt{2mE}/\hbar$, $k_j \equiv \sqrt{2m(E-\phi_j)}/\hbar$, $W_j = e^{ikw_j}$, $Z_j = e^{2ikz_j}$, and $\{s,c\}_j \equiv \{\sin, \cos\} k_j w_j$. In the Kronig-Penny limit, we take $w_j = 0$, $\phi_j = \pm\infty$ keeping $\phi_j w_j \equiv \tilde{\phi}_j$ constant. Matrix g_j reduces to

$$g_j = \begin{bmatrix} 1 \mp \zeta & \mp Z_j^* \zeta \\ \pm Z_j^* \zeta & 1 \pm \zeta \end{bmatrix} , \tag{A7}$$

where

$$\zeta = i \frac{m \tilde{\phi}_j}{k \hbar^2} . \tag{A8}$$

Setting $t_0 = 1$, $r_0 = r$, and $t_N = t$, $r_N = 0$, we find that the transmission coefficient t and the reflection coefficient r are given by

$$t=g_{22}^{-1}, \quad r=-g_{21}g_{22}^{-1} . \tag{A9}$$

The transmission of sound wave through layers of objects is described in the same fashion. When the sound velocity is c in the free space and c_j in the jth object, k and k_j are replaced by ω/c and ω/c_j in Eq. (A6).

C. Lattice vibration and heat conduction (Ref. 21)

We consider vibration of one-dimensional N lattice points described by

$$m_j\ddot{u}_j=-(k_{j-1}+k_j)u_j+k_{j-1}u_{j-1}+k_ju_{j+1}+\Delta_j , \tag{A10}$$

where $u_0=u_{N+1}=0$ and the end points $j=1$, N are under friction and Gaussian random forces,

$$\Delta_j=(\delta_{j,1}+\delta_{j,N})(-\lambda_j\dot{u}_j+f_j) . \tag{A11}$$

By choosing

$$\langle f_j(t)f_{j'}(t')\rangle=2kT_j\lambda_j\delta_{jj'}\delta(t-t') , \quad (\langle f_j(t)\rangle=0) \tag{A12}$$

we find that in equilibrium, i.e., $T_1=T_N=T$,

$$\langle \tfrac{1}{2}m_j\dot{u}_j^2\rangle=\tfrac{1}{2}kT . \tag{A13}$$

Thus Δ_j represents heat baths with temperature T_1 and T_N.

In order to survey the heat conduction through this harmonic chain, we rewrite (A10) in the matrix notation in the frequency domain $u=e^{-i\omega t}a$, as $\Phi a=\Delta$, where

$$\Phi_{ij}\equiv\delta_{i,j}(k_{j-1}+k_j-m_j\omega^2) -\delta_{i,j-1}k_{j-1}-\delta_{i,j+1}k_j . \tag{A14}$$

We define

$$d_{i,j}\equiv\frac{1}{\prod_{l=i}^{j}k_l}\det\begin{bmatrix}\Phi_{ii} & \cdots & \Phi_{ij}\\ \vdots & & \vdots\\ \Phi_{ji} & \cdots & \Phi_{jj}\end{bmatrix} . \tag{A15}$$

The iteration (4.1) is satisfied for

$$v_j=\sqrt{k_j}\begin{bmatrix}d_{i,j}\\ d_{i,j-1}\end{bmatrix} , \qquad g_j=\left[\frac{k_j}{k_{j-1}}\right]^{1/2}\begin{bmatrix}\dfrac{-m_j\omega^2+(k_{j-1}+k_j)}{k_j} & -\dfrac{k_{j-1}}{k_j}\\ 1 & 0\end{bmatrix} . \tag{A16}$$

From the known value of $d_{1,1}$, $d_{1,2}$, $d_{2,2}$, and $d_{2,3}$, we find the effective "initial" values,

$$d_{1,0}=1, \quad d_{1,-1}=0, \quad d_{2,0}=0, \quad d_{2,-1}=-\frac{k_1}{k_0} . \tag{A17}$$

The heat flux J is given as follows:

$$J=\frac{\lambda_1}{m_1}(kT_1-\langle m_1\dot{u}_1^2\rangle) \equiv(T_1-T_N)\int_0^\infty d\omega\, j(\omega) . \tag{A18}$$

One can find that $j(\omega)$ is given by[21]

$$j(\omega)\equiv\frac{2\lambda_1\lambda_N\omega^2}{k_N^2\pi}\frac{1}{\left[d_{1,N}-\omega^2\dfrac{\lambda_1\lambda_N}{k_1k_N}d_{2,N-1}\right]^2+\omega^2\left[\dfrac{\lambda_1}{k_1}d_{2,N}+\dfrac{\lambda_N}{k_N}d_{1,N-1}\right]^2} =\frac{2\omega^2\sigma_1\sigma_N}{\pi}\frac{1}{(g_{11}+\sigma_1\sigma_Ng_{22})^2+(\sigma_1g_{12}-\sigma_Ng_{21})^2} , \tag{A19}$$

where $\sigma_1\equiv\omega\lambda_1/k_0$ and $\sigma_N\equiv\omega\lambda_N/k_N$.

D. Spectral diffusion

Consider a spectral diffusion from the origin governed by the random walk equation[18,22]

$$\dot{P}_j=w_j(P_{j+1}-P_j)+w_{j-1}(P_{j-1}-P_j) \tag{A20}$$

for $j=1,\ldots,N$ and $P_0=P_{N+1}=0$. $P_j\equiv P(j,t|1,0)$ is the probability that one finds an excitation at site j at time t when it created on site 1 at time $t=0$. w_0 and w_N, denote absorption at both ends of the chain. Although these can be set to be zero, we keep them for the sake of simple presentation of transfer matrices.

It is convenient to write the random walk equations in the Laplace domain. The Laplace transform of P_j,

$$\tilde{P}_j\equiv\tilde{P}(j,\mu|1)=\int_0^\infty P(j,t|1,0)e^{-\mu t}dt \tag{A21}$$

obeys

$$(\mu+w_j+w_{j-1})\tilde{P}_j-w_j\tilde{P}_{j+1}-w_{j-1}\tilde{P}_{j-1}=\delta_{j,1} . \tag{A22}$$

Suppose now we observe the excitation at site 1 or site N, i.e., we look at P_1 or P_N, or their Laplace transform $\tilde{P}_1$ or $\tilde{P}_N$. The latters are given by

$$\tilde{P}_1=(D^{-1})_{11}, \quad \tilde{P}_N=(D^{-1})_{N1} , \tag{A23}$$

where an $N\times N$ matrix D is defined by

$$D_{mn}=(\mu+w_m+w_{m-1})\delta_{m,n} -w_{m-1}\delta_{m-1,n}-w_m\delta_{m+1,n} . \tag{A24}$$

We introduce a vector v_j by

$$v_j=\sqrt{w_j}\begin{bmatrix} d_{i,j} \\ d_{i,j-1}\end{bmatrix} \tag{A25}$$

with

$$d_{i,j}\equiv\frac{1}{\prod_{l=i}^{j} w_l}\det\begin{bmatrix} D_{ii} & \cdots & D_{ij} \\ \vdots & & \vdots \\ D_{ji} & \cdots & D_{jj}\end{bmatrix}. \tag{A26}$$

Then v_j satisfies Eq. (4.1) with

$$g_j=\left[\frac{w_j}{w_{j-1}}\right]^{1/2}\begin{bmatrix}\dfrac{\mu+w_{j-1}+w_j}{w_j} & -\dfrac{\omega_{j-1}}{w_j} \\ 1 & 0\end{bmatrix}. \tag{A27}$$

From the known value of $d_{1,1}$, $d_{1,2}$, $d_{2,2}$, and $d_{2,3}$, we find the effective "initial" values,

$$\begin{aligned} &d_{1,0}=1,\quad d_{1,-1}=0\ , \\ &d_{2,0}=0,\quad d_{2,-1}=-\frac{w_1}{w_0}\ . \end{aligned} \tag{A28}$$

Using the determinant formula for the inverse matrix elements, one can easily show

$$\tilde{P}_1=\frac{g_{12}}{w_0 g_{11}} \tag{A29}$$

and

$$\tilde{P}_N=\frac{1}{\sqrt{w_0 w_N}\,g_{11}}\ . \tag{A30}$$

E. Lenses

Imagine a series of N coaxial lenses with focal lengths $f_1,\ldots,f_N$. Between f_j and f_{j+1} is a medium of refractive index n_j and thickness l_j. Take an object at distance a_0 (on the axis) to the left of f_1 ($a_0<0$). The lens f_1 creates its image at distance b_1 to the right, which is at distance a_1 to the left of f_2 and so forth. The relation between a's and b's are

$$a_j=b_j-l_j,\quad -\frac{n_{j-1}}{a_{j-1}}+\frac{n_j}{b_j}=\frac{1}{f_j}\ , \tag{A31}$$

Therefore $z_j\equiv a_j$ follows Eq. (4.1), where

$$g_j\equiv\left[\frac{n_j}{n_{j-1}}\right]^{1/2}\begin{bmatrix}1-\dfrac{l_j}{n_j f_j} & -\dfrac{n_{j-1}}{n_j}l_j \\ \dfrac{1}{n_j f_j} & \dfrac{n_{j-1}}{n_j}\end{bmatrix}. \tag{A32}$$

The variable a_N and l_N are unphysical (dummy) variables.

This system is characterized by the effective focal length f_{eff} and effective lengths of the system h_1 and h_2 defined by the following relation:

$$\frac{1}{f_{\text{eff}}}=-\frac{n_0}{a_0+h_1}+\frac{n_N}{b_N-h_2}\ . \tag{A33}$$

We find

$$\begin{aligned} f_{\text{eff}}&=\frac{1}{\sqrt{n_0 n_N}\,g_{21}}\ , \\ h_1&=\frac{1}{g_{21}}\left[g_{22}-\left[\frac{n_0}{n_N}\right]^{1/2}\right], \\ h_2&=\frac{1}{g_{21}}\left[g_{11}-\left[\frac{n_N}{n_0}\right]^{1/2}\right]+l_N\ . \end{aligned} \tag{A34}$$

F. Optical layers

Take N layers of thickness $h_1,\ldots,h_N$ with refractive indices $n_1,\ldots,n_N$ (ordered from left to right). We take the normal incident light from left with wavelength λ. We denote the right-going electric field in the jth layer, at the boundary with the $(j+1)$th layer E_j^+. Similarly, that of the left-going field is denoted E_j^-. The variable

$$v_j\equiv\begin{bmatrix}E_j \\ iH_j\end{bmatrix}\equiv\begin{bmatrix}E_j^+ + E_j^- \\ in_j(E_j^+ - E_j^-)\end{bmatrix}, \tag{A35}$$

and $z_j\equiv E_j/iH_j$ are continuous across the boundary and obeys Eq. (4.1), where

$$g_j\equiv\begin{bmatrix}\cos k_j & n_j^{-1}\sin k_j \\ -n_j\sin k_j & \cos k_j\end{bmatrix} \tag{A36}$$

($k_j\equiv 2\pi n_j h_j/\lambda$). The amplitude of the reflected light r and that of the transmitted light t is obtained from

$$v_0=\begin{bmatrix}1+r \\ in_0(1-r)\end{bmatrix},\quad v_N=\begin{bmatrix}t \\ in_{N+1}t\end{bmatrix}. \tag{A37}$$

We find that

$$\begin{aligned} r&=-\frac{n_{N+1}g_{11}+n_0 g_{22}-i(n_0 n_{N+1}g_{12}-g_{21})}{n_{N+1}g_{11}-n_0 g_{22}+i(n_0 n_{N+1}g_{12}+g_{21})}\ , \\ t&=\frac{2n_0}{n_{N+1}g_{11}+n_0 g_{22}-i(n_0 n_{N+1}g_{12}-g_{21})}\ . \end{aligned} \tag{A38}$$

G. Ladder of two-port circuits

Take series of two-port networks, where each network is characterized by the *chain matrix* g_j. Then the vector

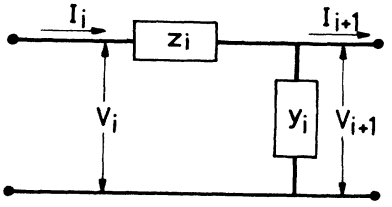

FIG. 12. Two-port circuit. y_j and z_j are impedances. A vector of the current I_j and the voltage V_j is transformed by an $SL(2,C)$ defined by Eq. (A40).

$$v_j \equiv \begin{bmatrix} V_j \\ I_j \end{bmatrix} \tag{A39}$$

of the potential V_j and the current I_j satisfies Eq. (4.1). The chain matrix for a reciprocal network satisfies $\det g = 1$. For example, a simple circuit illustrated in Fig. 12 is characterized by

$$g_j = \begin{bmatrix} 1 & -z_j \\ -y_j & 1+z_j y_j \end{bmatrix}, \tag{A40}$$

where y_j and z_j are impedances. The total short-circuit admittance matrix Y is given by

$$\begin{bmatrix} -I_N \\ I_0 \end{bmatrix} = Y \begin{bmatrix} V_N \\ V_0 \end{bmatrix}, \qquad Y = \frac{1}{g_{12}} \begin{bmatrix} -g_{22} & 1 \\ 1 & -g_{11} \end{bmatrix}. \tag{A41}$$

Similarly, the open-circuit impedance matrix Z is given by

$$Z \equiv Y^{-1} = -\frac{g_{12}}{g_{21}} \begin{bmatrix} g_{11} & 1 \\ 1 & g_{22} \end{bmatrix}. \tag{A42}$$

Various transfer functions to characterize the circuit are obtained from Y and Z.

---

*Permanent address: Physics Department, Kyoto University, Kyoto 606, Japan.

[1]D. Hofstadter, Phys. Rev. B **14**, 2239 (1976).
[2]D. Shechtman, I. Blech, D. Gratias, and J. W. Cahn, Phys. Rev. Lett. **53**, 1951 (1984).
[3]D. Levine and P. J. Steinhardt, Phys. Rev. Lett. **53**, 2477 (1984); Phys. Rev. B **34**, 596 (1986).
[4]*The Physics of Quasicrystals,* edited by P. J. Steinhardt and S. Ostlund (World-Scientific, Singapore, 1987).
[5]R. Merlin, K. Bajema, R. Clarke, F.-Y. Juang, and P. K. Bhattacharya, Phys. Rev. Lett. **55**, 1768 (1986); T. Odagaki and L. Friedman, Solid State Commun. **57**, 915 (1986).
[6]J. Harvey, G. Moore, and C. Vafa (unpublished).
[7]V. Elser and C. Henley, Phys. Rev. Lett. **55**, 2883 (1985).
[8]T. Odagaki and H. Aoyama, Phys. Rev. Lett. **61**, 775 (1988).
[9]N. G. de Bruijn, Kon. Nederl. Akad. Wetensch. Proc. Ser. A **84**, 27 (1981); J. E. S. Socolar and P. J. Steinhardt, Phys. Rev. B **34**, 617 (1986).
[10]We can also transform 0 to 0 and 1 to 1 by $k'=2k+i$ and $i'=k+i$. Pairs are transformed as 00→010, 01→0101, 10→110, and 11→1101. The units are, of course, transformed as 0→10 and 1→101, the same as in Eq. (2.14).
[11]J. P. Lu and J. L. Birman, J. Phys. (Paris) Colloq. Suppl. **7**, C3-251 (1986); M. Duneau and K. Katz, Phys. Rev. Lett. **54**, 2688 (1985); P. A. Kalugia, A. Kitaev, and L. Levitov, Pis'ma Zh. Eksp. Theor. Fiz. **41**, 119 (1985) [JETP Lett. **41**, 145 (1985)]; R. Zia and W. Dallas, J. Phys. A **18**, L314 (1985).
[12]E. H. Lieb and D. C. Mattis, *Mathematical Physics in One Dimension* (Academic, New York, 1966).
[13]J. B. Sokoloff, Phys. Rep. **126**, 189 (1985).
[14]K. Ishii, Prog. Theor. Phys. Suppl. **53**, 77 (1973).
[15]J. B. Sokoloff, Phys. Rev. B **22**, 5823 (1980); M. Khomoto, L. P. Kadanoff, and C. Tang, Phys. Rev. Lett. **50**, 1870 (1983); B. Sutherland and M. Khomoto, Phys. Rev. B **36**, 5877 (1987).
[16]J. B. Sokoloff, Phys. Rev. B **25**, 5901 (1982); M. Khomoto and J. R. Banavar, *ibid.* **34**, 563 (1986); T. Nagatani, *ibid.* **32**, 2049 (1985); J. P. Lu, T. Odagaki, and J. L. Birman, *ibid.* **33**, 4809 (1986); K. Machida and M. Fujita, *ibid.* **34**, 7367 (1986); T. Ninomiya, J. Phys. Soc. Jpn. **55**, 3709 (1986); T. Odagaki and D. Nguyen, Phys. Rev. B **33**, 2184 (1986); J. M. Luck and D. Petritis, J. Stat. Phys. **42**, 289 (1986); M. Fujita and K. Machida, J. Phys. Soc. Jpn. **56**, 1470 (1987).
[17]M. Khomoto, B. Sutherland, and K. Iguchi, Phys. Rev. Lett. **58**, 2436 (1987).
[18]M. Khanta and R. B. Stinchcombe, J. Phys. A **20**, 495 (1987).
[19]R. Landauer, Philos. Mag. **21**, 683 (1970).
[20]N. W. Achcroft and N. D. Mermin, *Solid State Physics* (Holt, Rinehart, and Winston, Philadelphia, 1976).
[21]A. Casher and J. L. Lebowitz, J. Math. Phys. **12**, 1701 (1971).
[22]S. Alexander, J. Bernasconi, and R. Orbach, Phys. Rev. B **17**, 4311 (1978); S. Alexander, J. Bernasconi, W. R. Schneider, and R. Orbach, Rev. Mod. Phys. **53**, 175 (1981).